Environmental Science and Pollution Research (2022) 29:79816–79829
https://doi.org/10.1007/s11356-021-17551-x

ADSORPTION (AND CATALYSIS OR PHOTOCATALYSIS) APPLIED TO ENVIRONMENTAL PROTECTION

Uranium biosorption by hydroxyapatite and bone meal: evaluation of process variables through experimental design

Tamires Watanabe[1] · Sabine Neusatz Guilhen[1] · Júlio Takehiro Marumo[1] · Rodrigo Papai de Souza[2] · Leandro Goulart de Araujo[1]

Received: 9 August 2021 / Accepted: 11 November 2021 / Published online: 23 November 2021
© The Author(s), under exclusive licence to Springer-Verlag GmbH Germany, part of Springer Nature 2021

Abstract

Biosorption has been examined for the treatment of aqueous solutions containing uranium, a radiotoxic pollutant. Nevertheless, the evaluation of the role of process variables by experimental design on the use of hydroxyapatite and bone meal as biosorbents for uranium has not yet been previously addressed. In this study, the effects of adsorbent dosage (M), initial uranium concentrations ($[U]_0$), and solution pH were investigated, using a two-level factorial design and response surface analysis. The experiments were performed in batch, with $[U]_0$ of 100 and 500 mg L^{-1}, pH 3 and 5, and adsorbent/uranium solution ratios of 5 and 15 g L^{-1}. Contact time was fixed at 24 h. Removal rates were higher than 88%, with a maximum of 99% in optimized conditions. $[U]_0$ and M were found to be the most influential variables in U removal in terms of adsorption capacity (q). The experiments revealed that bone meal holds higher adsorption capacity (49.87 mg g^{-1}) and achieved the highest uranium removal (~ 100%) when compared to hydroxyapatite ($q = 49.20$ mg g^{-1}, removal = 98.5%). The highest value of q for both biomaterials was obtained for $[U]_0 = 500$ mg L^{-1}, pH 3, and $M = 5$ g L^{-1}. Concerning the removal percentage, bone meal achieved the best performance for $[U]_0 = 500$ mg L^{-1}, pH 3, and $M = 15$ g L^{-1}. Further experiments were made with real radioactive waste, resulting in a high uranium adsorption capacity for both materials, with 22.11 mg g^{-1} for hydroxyapatite and 22.08 mg g^{-1} for bone meal, achieving uranium removal efficiencies higher than 99%.

Keywords Adsorption of radionuclides · Biomaterials · Two-level factorial design · Radioactive waste · Response surface methodology

Responsible Editor: Tito Roberto Cadaval Jr.

✉ Leandro Goulart de Araujo
lgoulart@alumni.usp.br

Tamires Watanabe
tamireswatanabe@gmail.com

Sabine Neusatz Guilhen
snguilhen@ipen.br

Júlio Takehiro Marumo
jtmarumo@ipen.br

Rodrigo Papai de Souza
rodrigopapai@ipt.br

[1] Instituto de Pesquisas Energéticas e Nucleares (IPEN-CNEN/SP), Av. Prof. Lineu Prestes, São Paulo 05508-000, Brazil

[2] Instituto de Pesquisas Tecnológicas do Estado de São Paulo (IPT), Av. Prof. Almeida Prado, SP, São Paulo 532 – 05508-901, Brazil

Introduction

The presence of uranium in aqueous streams is of major radioecological importance, mainly because of its persistence in the environment over long periods. Sources of possible uranium contamination are numerous, including mineral mining, smelting, nuclear fuel generation, and nuclear research (Guilhen et al. 2019). Furthermore, given the growing demands for electric energy generation in the last decades, uranium-containing nuclear wastes have dramatically increased with the ascension of the nuclear power industry (Kahouli 2011).

Several methods have been specifically developed for uranium extraction from aqueous solutions (Wang and Zhuang 2019; Chen et al. 2020) such as covalent binding (Chen et al. 2013), ion-exchange (Rosenberg et al. 2016; Foster et al. 2020), electrostatic attraction (Zhao et al. 2018), surface complexation (Curtis et al. 2004; Davis et al. 2004; Coutelot

et al. 2018), and Van der Waal's forces (Sprynskyy et al. 2011). New and alternative processes are constantly being developed, aiming at removing radionuclides from aqueous solutions and also in overcoming known issues of the conventional treatment methods, such as the associated high costs and the generation of higher volumes of liquid waste resulting from these treatments (Das 2010, 2012).

Biosorption can be defined as the use of a biosorbent in the uptake of metal(loid) ions from aqueous environments. Examples of such biomaterials are algae, bacteria, yeast, fungi, plant leaves, and root tissues. Biosorption has many advantages, e.g., low capital and operating costs, selective removal of metals, the possibility of biosorbent regeneration and metal recovery, rapid kinetics of adsorption and desorption, and no sludge generation (Abbas et al. 2014). In this context, many biomaterials have been extensively studied for the removal of uranium from aqueous solutions (Wang and Chen 2009), including biomasses such as rice stem (Zhang et al. 2019), *Solanum incanum* leaves (Bakather et al. 2020), *Eichhornia crassipes* (Yi et al. 2016), macrophytes (Vieira et al. 2019), coconut fiber (Ferreira et al. 2018), coffee and rice husks (Ferreira et al. 2020); microorganisms such as *Saccharomyces cerevisiae* (Chen et al. 2020; Zhang et al. 2020; Wang and Chen 2006), *Penicillium piscarium* (Coelho et al. 2020), *Penicillium citrinum* (Pang et al. 2011), *Aspergillus fumigatus* (Wang et al. 2010), and biochars such as the ones derived from macauba (Guilhen et al. 2021), eucalyptus wood (Mishra et al. 2017), *Opuntia ficus indica* (Hadjittofi and Pashalidis 2014), rice straw (Dong et al. 2017; Yakout et al. 2018), bone (Ashry et al. 2016), and rice husk (Wang et al. 2018).

However, the use of bone meal for the removal of uranium from radioactive aqueous solutions has been scarcely investigated as a biosorbent. In this study, the bone meal was used for the first time, in a comprehensive experimental investigation, as a biosorbent for U. Hydroxyapatite is derived from bone and was used in this study as a traditional biosorbent, allowing a comparative evaluation of both materials. There are yet no reports of these materials in the literature regarding the treatment of real radioactive waste. Moreover, the empirical models generated from the experimental design reported in this study are original, especially those obtained for the bone meal.

In the context of radioactive waste treatment, good mechanical properties are a very important characteristic of the biosorbent, especially if the final goal is the solidification of the biomass waste (Bayoumi and Saleh 2018; Saleh et al. 2020). This will further impact the conditioning of the waste into a stable solid form which will allow immobilization and containment of the radioactive content for the necessary time (Bayoumi et al. 2013). The application of bone meal is attractive and advantageous because it is economically feasible in comparison with commercial adsorbents (Satir et al. 2021). It consists of a natural, abundant, substance that contains a large amount of calcium phosphate in the form of hydroxyapatite ($Ca_{10}(PO_4)_6(OH)_2$) (Paterlini et al. 2020).

Phosphate-derived materials, such as hydroxyapatite, have been extensively studied for their efficiency to extract uranium from the aqueous phase owing to their adsorption capability, which has been ascribed to the surface complexation and mineralization of phosphate with uranium (Kong et al. 2020). It can also be used to remove radionuclides from liquid radioactive waste generated in many industrial and research activities (Kim et al. 2017; Ahmed et al. 2021; Ouassel et al. 2021). Given the high potential of hydroxyapatite, this biomaterial may be able to significantly remove hazardous radionuclides, heavy metals, and organic substances from radioactive liquid waste. Previous research has indicated that hydroxyapatite alone is capable to efficiently remove thorium from aqueous solutions (Ferreira et al. 2015). Furthermore, studies indicate that radionuclides such as $^{90}Sr^{2+}$ (Kim et al. 2019), $^{208}Tl^{+}$, $^{226}Ra^{2+}$, $^{212}Bi^{3+}$, and $^{228}Ac^{3+}$ (Akkaya 2012) were also adsorbed by hydroxyapatite.

In this study, a full two-level factorial design is applied to evaluate the effect of three experimental variables—solution's initial concentration, pH, and adsorbent dosage—and their interactions on the removal percentage and adsorption capacity of bone meal and hydroxyapatite aiming to extract uranium from contaminated solutions. To the best of our knowledge, the influence of these variables on uranium removal through these biosorbents, especially bone meal, has not been previously investigated in such a detailed approach based on experimental design and response surface methodologies. Furthermore, both materials were tested, for the first time, as uranium biosorbents in a complex liquid radioactive organic waste from a nuclear reactor.

Materials and methods

Biosorbents

Bone meal (Fênix Indústria e Comércio de Fertilizantes, Brazil) was purchased in the local market, and hydroxyapatite was produced at the Materials Science and Technology Center of the Nuclear and Energy Research Institute (IPEN-CNEN/SP, Brazil). There was no pre-conditioning of the materials, besides grounding and sieving to obtain particle sizes between 0.297 mm and 0.125 mm. Subsequently, they were stored in glass vials in the laboratory for later use.

Synthetic and radioactive waste solutions

Synthetic solutions of uranium were prepared by diluting the uranyl nitrate ($UO_2(NO_3)_2.6H_2O$) stock solution in distilled

water. The initial pH of the prepared solution was 2.90, further adjusted to the desired pH values, 3 or 5, by adding either 1 mol L^{-1} nitric acid solution (Merck, Brazil) or 1 mol L^{-1} sodium hydroxide solution (Merck, Brazil). These values were selected because of the uranium speciation (Fig. S1 in Supplementary Information). The chemical equilibrium calculation was made in the HYDRA-MEDUSA software (Puigdomenech 2006). At this pH range, most of the uranium ions in the solution are in the form of non-complexed free uranyl ions (UO_2^{2+} $UO_2NO_3^{+}$) (Younes et al. 2018). After exploratory results, synthetic solutions with initial uranium concentrations ($[U]_0$) of 100 and 500 mg L^{-1}, pH 3 and 5, and adsorbent dosages of 5 and 15 g L^{-1} were selected for evaluation.

Experiments were also conducted with real liquid organic radioactive waste (LORW) of research and development activities from IPEN's IEA-R1 research reactor. More information on the characteristics of this waste is provided elsewhere (Ferreira et al. 2013).

The radioactive waste is composed of water; ethyl acetate (196 mg L^{-1}); tributyl phosphate (227 mg L^{-1}); [U(total)] ($(2.226 \pm 0.014) \times 10^2$ mg L^{-1}); and many other radionuclides (Ferreira et al. 2013). The pH value is about 3 since there is a significant amount of nitric acid in the liquid waste.

Biosorption experiments

Twenty-milliliter borosilicate glass vials with screw caps containing the solution and the biosorbent were stirred (130 rpm) at a controlled temperature (25 ± 2 °C) in an orbital shaker incubator (model BT 400, Biotech, Brazil). The evaluation of the role of process variables was made with 0.05 and 0.15 g of the adsorbents, which were suspended in 5 mL of uranium aqueous solutions (100 and 500 mg L^{-1}) and were kept in contact for 24 h. The supernatant was separated from each biosorbent by a vacuum filtration system (Model WP6211560, Millipore, USA) with paper filters (slow filtration with an ash content ≤ 0.009%, GE Healthcare, USA). Total uranium concentration was determined in the adsorbate solutions, for synthetic and LORW, by an iCAP 7400 Thermo ICP OES (Thermo Fisher Scientific™, Waltham, EUA) using a linear calibration curve at 409.014 nm between 0.05 and 5.00 mg L^{-1} ($R^2 = 0.9999$). The uptake amount of uranium onto the biomaterial was calculated using equation Eq. (1).

$$q = \frac{(C_0 - C_{(t)})V}{m} \quad (1)$$

where q is the uptake of uranium (mg g^{-1}), C_0 is the $[U]_0$ in solution (mg L^{-1}), C is the equilibrium concentration in solution (mg L^{-1}) in a given time t, V is the volume of solution (L), and m is the mass of the biosorbent (g).

The removal percentage, R (%), was determined through the following equation:

$$R(\%) = 100\frac{(C_0 - C_{(t)})}{C_0} \quad (2)$$

where R is the efficiency of extraction or retention percentage, C_0 (mg L^{-1}) is the initial concentration of U, and $C_{(t)}$ (mg L^{-1}) represents the uranium concentration at time t.

SEM/EDS analysis

Scanning electron microscopy (SEM) images of the biosorbents were obtained with a Hitachi TM-3000 (Tokyo, Japan) tabletop microscope. Energy-dispersive X-ray spectroscopy (EDS) data was also collected with this equipment, with a tungsten source and acceleration voltages of 5 and 15 kV and electron beam resolution of 30 nm. The samples were dried in an oven (model 78,532, WTC Binder, Germany), at a controlled temperature (105 ± 2 °C) for 24 h. Double-sided carbon adhesives were used to attach the material onto the SEM stub. Images were obtained with magnification from 500 to 1500 times. SEM allowed morphological comparison between both raw biosorbents and their loaded versions, in the following conditions: $[U]_0 = 500$ mg L^{-1}; $[pH]_0 = 5$; $M = 15$ g L^{-1}; contact time = 30 min.

Two-level factorial design

The adsorption experiments were performed based on the $n = 2^k$ equation, where n is the total of experiments, and k is the number of variables. To determine the importance of each process variable in terms of maximizing uranium removal, a full factorial design was set up considering the solution's initial concentration (C_i), pH, and the biosorbents dosage (M), as shown in Table 1 (see also Supplementary Information for the illustration, Fig. S2).

In summary, the effect of the variables was evaluated using the 2^3 factorial design, performed in duplicate (total of 16 experimental runs), and assessed according to each parameter's low and high levels, represented by (-1) and (+1), respectively.

The experimental design, as well as the statistical analysis, was processed using the RStudio Software (R Core Team 2021) with the package PID (Dunn 2021). Table 2 shows

Table 1 Real and coded variables for *Ci*, pH, and *M*

Variables	Factor code	Low level (-1)	High level (+1)
C_i(mg L^{-1})	A	100	500
pH	B	3	5
M (g L^{-1})	C	5	15

Table 2 Matrix of the full two-level factorial design

Test	$[U]_0$ (mg L^{-1})	pH	M (g L^{-1})
1	100 (-1)	3 (-1)	5 (-1)
2	500 (+1)	3 (-1)	5 (-1)
3	100 (-1)	5 (+1)	5 (-1)
4	500 (+1)	5 (+1)	5 (-1)
5	100 (-1)	3 (-1)	15 (+1)
6	500 (+ 1)	3 (-1)	15 (+1)
7	100 (-1)	5 (+1)	15 (+1)
8	500 (+1)	5 (+1)	15 (+1)

the matrix of the full factorial design of each test with their respective real and coded values. The analysis of variance (ANOVA) of data was carried out at a 95% confidence level to evaluate the interactions of the independent variables and the main effects on the removal percentage of uranium and adsorption capability.

The effect of each factor and its interactions were evaluated in this work. The result of the full factorial design is an adjusted linear equation that describes the value of the outcome as a function of the factors and their interactions, as follows:

$$Y = \beta_0 + \beta_1 A + \beta_2 B + \beta_3 C + \beta_4 AB + \beta_5 AC + \beta_6 BC + \beta_7 ABC \quad (3)$$

where Y is the outcome, β_0 represents the intercept, β_i is the regression coefficient related to the interactions, and the main variables "A" is the solution's initial concentration (mg L^{-1}), "B" is the pH value, and "C" is the adsorbent dosage (g L^{-1}). Variables A, B, and C, each represent the main effect, referring to the primary variables of interest. Variables AB, AC, BC, and ABC represent the interaction effects.

Four dependent variables were evaluated: Y_1 stands for uranium removal (%) by hydroxyapatite, Y_2 is the adsorption capacity for hydroxyapatite (mg g^{-1}), Y_3 is the uranium removal (%) for bone meal, and finally, Y_4 represents the adsorption capacity for the bone meal (mg g^{-1}).

Results and discussion

Morphological analysis

Although the apparent density of hydroxyapatite (1.0298 ± 0.0001 g mL^{-1}) and bone meal (0.9089 ± 0.0001 g mL^{-1}) are somewhat similar, SEM analysis indicated a rather different morphology of these materials. Visual surface transformations during uranium adsorption are shown in the micrographs in Figs. 1 and 2 for the bone meal and hydroxyapatite, respectively. The micrographs compare the material before and after the adsorption process, applying the conditions described in the "SEM/EDS analysis" section.

Micrograph images of hydroxyapatite and bone meal were captured using particle sizes between 0.125 and 0.297 mm. Figure 1a and Fig. 2a correspond to the micrographs of both materials before the batch experiments were undertaken, evidencing their irregular surface. Nevertheless, hydroxyapatite presents a more uniform structure compared to the bone meal. The micrographs (Fig. 1c and Fig. 2c) show that after 30 min of contact with the U solution, both biomaterials' surfaces were modified as seen by the decreased presence of interstices.

EDS analysis of the raw materials revealed that they possess a similar chemical composition (Fig. 1b and Fig. 2b). Both raw materials contain calcium, phosphorus, and sulfur. The analysis demonstrated that bone meal has a more significant amount of calcium (41.1%) than hydroxyapatite (28.5%). According to Liu et al. (2016), uranyl ions can react with the calcium surface sites present in hydroxyapatite through ion exchange. In this case, better performance for the bone meal is expected since there may be a higher availability of calcium sites for this material, as indicated by EDS analysis. Oxygen content was similar for both materials (27%). Phosphorus content was also alike, with 2.5% for hydroxyapatite and 4.2% for bone powder. Bone meal (2.1%) showed a fairly superior amount of aluminum than hydroxyapatite (0.1%). After the adsorption experiments, a certain amount of uranium was found attached to the biosorbents surface (Fig. 1d and Fig. 2d).

Experimental data

In the following paragraphs, the results of biosorption of uranium in synthetic solutions are discussed by the factorial experimental design. Afterward, the results on the biosorption of U(total) in a LORW are presented. Table 3 shows the conditions of the biosorption experiments, which were performed at different $[U]_0$, pH, and adsorbents dosages. The measured responses are also given.

Removal rates for hydroxyapatite comprised a range between 88.9 and 98.5% depending on the experimental condition, whereas bone meal indicated increased rates with more than 99% of uranium removal for all experimental conditions. On the other hand, adsorption capacities were very similar (approx. 50 mg g^{-1}), with the highest values obtained in Run 2 ($[U]_0 = 500$ mg L^{-1}; pH = 3; $M = 5$ g L^{-1}) and Run 4 ($[U]_0 = 500$ mg L^{-1}; pH = 5; $M = 5$ g L^{-1}) for both materials. A comparison between these results and those obtained with the LORW will be given further.

pH increased in most of the experiments after 24 h of the mixtures (Fig. S3), with the maximum mean pH value of 7.18 obtained in Run 8H ("H" for hydroxyapatite). Runs 3H and 4B ("B" for bone meal) indicated almost no

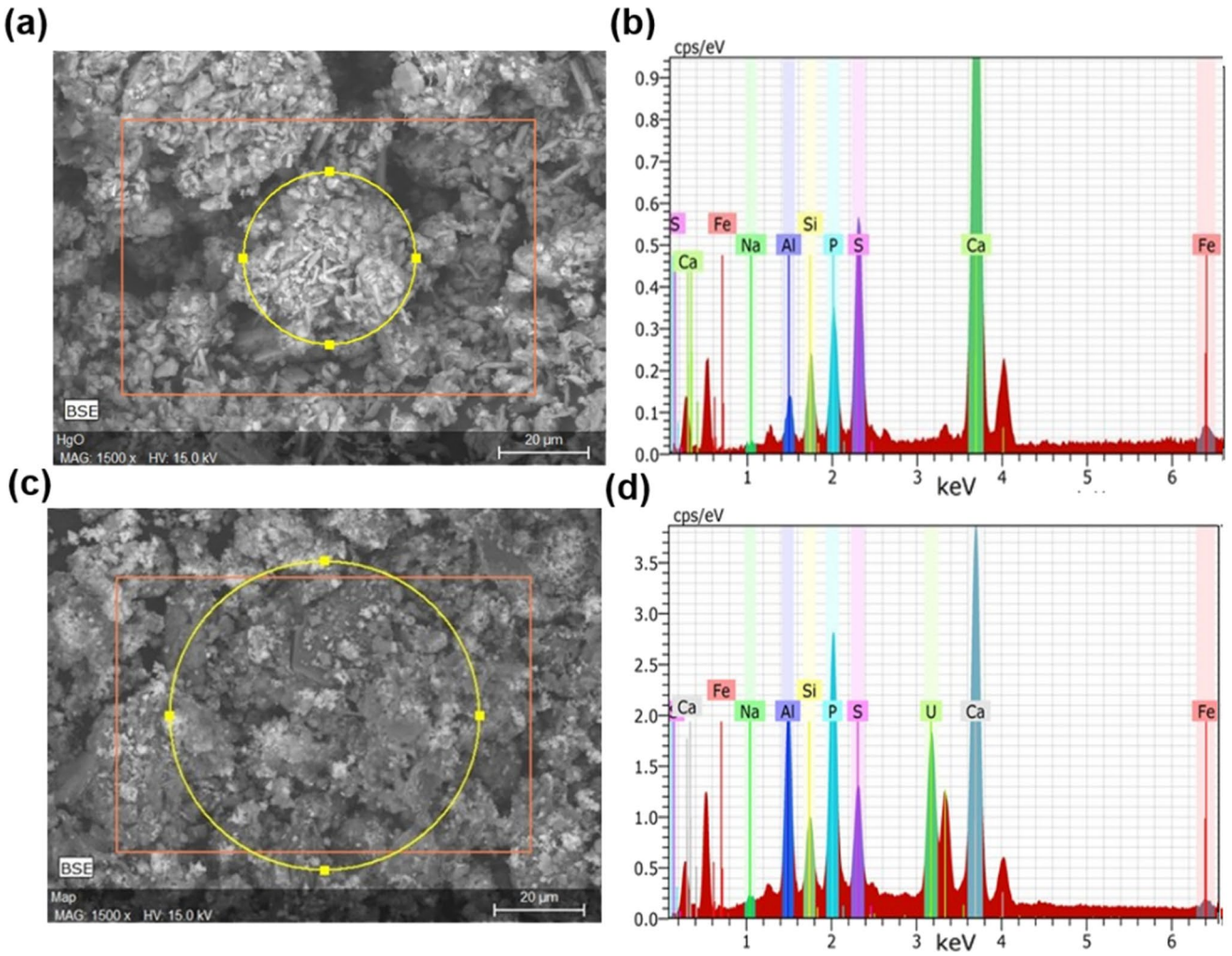


Fig. 1 SEM images and EDS spectra of bone meal. **a** Micrograph of the raw material; **b** EDS of the raw material; **c** Micrograph after 30 min in contact with the uranium-contaminated solution; **d** EDS after 30 min in contact with the uranium-contaminated solution

difference in terms of pH after 24 h. Both Runs are the ones conducted with the initial pH 5 and $M = 5$ g L^{-1}, indicating possible stability of the process. Run 3B, also with initial pH 5 and $M = 5$ g L^{-1}, presented a slightly lower pH after 24 h when compared to its initial pH, also observed in Run 4B. According to Xiong et al. 2021, three mechanisms may be involved in the removal of U(IV) by hydroxyapatite adsorption, dissolution–precipitation, and ion-exchange. The extent of each mechanism in the mixture of calcium phosphate compounds such as bone meal or hydroxyapatite and uranium in aqueous solutions is complex, but pH changes over time may bean indicative of which mechanisms are influencing the most in the adsorbent-adsorbate interaction. Given that pH increased in most runs, for both materials, the dissolution–precipitation was possibly the primary process during the experimental trials. In this case, a portion of these materials would have dissolved due to the acidic conditions of the solutions, releasing Ca^{2+} and PO_4^{3-} ($Ca_{10}(PO_4)_6(OH)_2 \rightleftharpoons 10Ca^{2+} + 6PO_4^{3-} + 2OH^-$) that may have reacted with U(VI). This reaction could have formed a new phase of $Ca(UO_2)_2(PO_4)_2 \cdot 3H_2O$.

Full factorial experimental design for the uranium removal by hydroxyapatite and bone meal

The responses selected to evaluate uranium biosorption were U removal (Y_1 for hydroxyapatite, Y_3 for bone meal, %) and adsorption capacity (Y_2 for hydroxyapatite, Y_4 for bone meal, mg g^{-1}). The statistical summary (Tables S1 and S2) and the Pareto charts (Fig. 3) show the significant effects on the responses at the 95% confidence level (p values < 0.05) for the experiments with hydroxyapatite.

The length of each bar indicates the absolute value of the estimated effects, which is important to determine the main variables on uranium removal. Depending on the response variable, Y_1 or Y_2, the effects of the independent variables

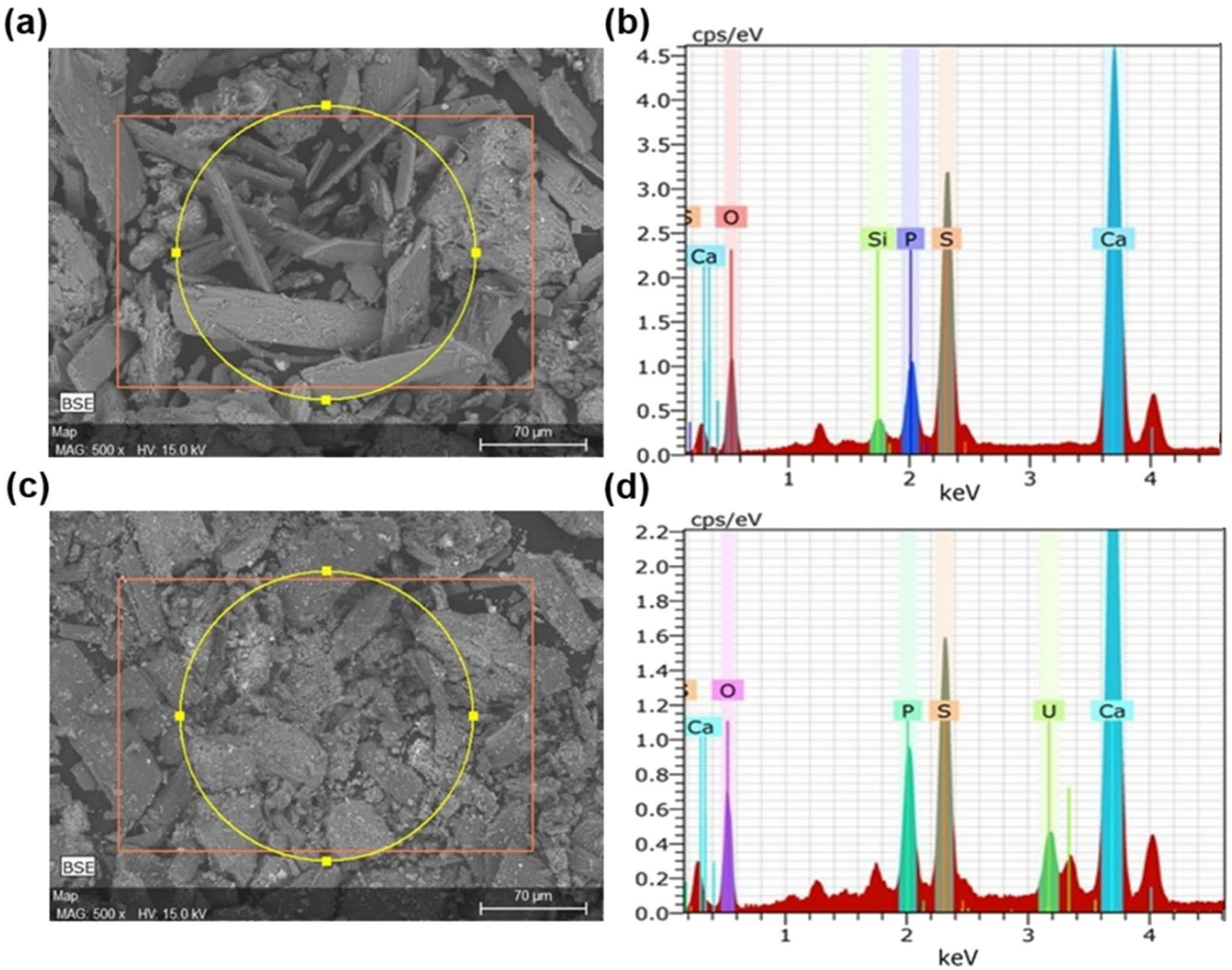


Fig. 2 SEM images and EDS spectra of hydroxyapatite. **a** Micrograph of the raw material; **b** EDS of the raw bone meal; **c** micrograph after 30 min in contact with the uranium-contaminated solution; **d** EDS after 30 min in contact with the uranium-contaminated solution

Table 3 Conditions and results of the biosorption experiments

Run no	$[U]_0$ (mg L^{-1})	pH	M (g L^{-1})	Hydroxyapatite		Bone meal	
				Y_1 (%)	Y_2 (mg g^{-1})	Y_3 (%)	Y_4 (mg g^{-1})
1	100 (-1)	3 (-1)	5 (-1)	94.4	9.4	99.6	10.0
2	500 (+1)	3 (-1)	5 (-1)	98.5	49.2	99.9	49.9
3	100 (-1)	5 (+1)	5 (-1)	95.0	9.5	99.8	10.0
4	500 (+1)	5 (+1)	5 (-1)	97.9	48.9	99.5	49.6
5	100 (-1)	3 (-1)	15 (+1)	88.9	3.0	99.8	3.3
6	500 (+1)	3 (-1)	15 (+1)	95.4	15.9	99.9	16.7
7	100 (-1)	5 (+1)	15 (+1)	92.4	3.1	99.7	3.3
8	500 (+1)	5 (+1)	15 (+1)	91.4	15.2	99.9	16.6

Y_1 U removal (%) by hydroxyapatite; Y_2 adsorption capacity for hydroxyapatite (mg g^{-1}); Y_3 U removal (%) for the bone meal; Y_4 represents the adsorption capacity for the bone meal (mg g^{-1})

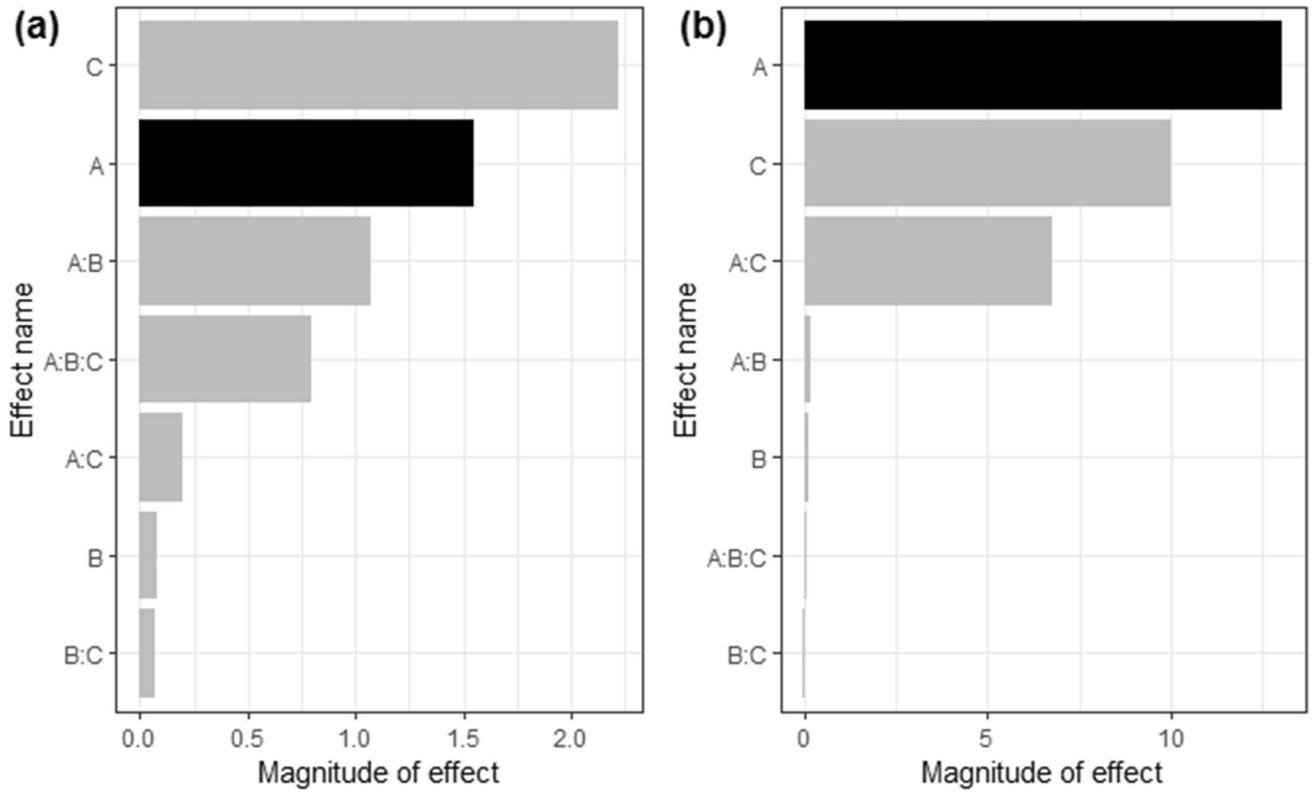


Fig. 3 Pareto plots for the experiments with hydroxyapatite: (gray fill) negative effect, (black fill) positive effect. **a** Removal percentage; **b** adsorption capacity. A = $[U]_0$, B = pH, C = M (g L^{-1})

(A, B, or C) and their interactions provided contrasting outcomes.

When it comes to removal percentage, we found that adsorbent dosage (C), the interaction between $[U]_0$:pH (B:C) and the three-variable interaction (A:B:C), contribute to a higher or lower degree to decrease uranium removal (Y_1) (Table S1). On the other hand, increased $[U]_0$ provided higher uranium removals, highlighting that higher uranium amounts did not impair the adsorption of this element by the hydroxyapatite (See Table S2). This is an indication that a higher availability of uranium ions may facilitate the adsorption process with the hydroxyapatite. Only when pH and adsorbent dosage were kept at 5 and 15 g L^{-1}, respectively, the uranium removal rate was diminished (Run 7 vs. Run 8).

In terms of adsorption capacity (q_{exp}, Y_2), the only significant effects were the positive effect of $[U]_0$, the negative effect of M, and their interaction (See also Supplementary Information, Table S2). The uppermost level of factor A ($[U]_0$ (500 mg L^{-1})) resulted in an increased adsorption capacity of the hydroxyapatite (See Table 2), reaching values 3 to 5 times superior when compared to the lower level of $[U]_0$ (100 mg L^{-1}).

The effect of the $[U]_0$ on the responses is so critical that it may hide the effect of the other independent variables or their interactions. Response surface models were then considered to search for the best domain in which uranium biosorption would be paramount. Table 4 lists the values of the fitted coefficients of the response surface model for the biosorption process with hydroxyapatite, and Fig. 4c and 4d show two and three-dimensional contour plots for the response variables Y_1 and Y_2.

Table 4 The empirical models generated from the data of the full factorial experimental design. Only the significant independent variables were considered in these equations. For more details, refer to Table 3

Biosorbent	Equation
Hydroxyapatite	$Y_1 = 94.23 + 1.55A - 2.22C - 1.07AB - 0.80ABC$
	$Y_2 = 19.26 + 13.02A - 9.98C - 6.76AC$
Bone meal	$Y_3 = 99.78 + 0.05A + 0.08C - 0.09AB + 0.08ABC$
	$Y_4 = 19.91 + 13.27A - 9.93C - 6.61AC$

Figure 4a illustrates that to obtain the highest removal percentage for hydroxyapatite, $[U]_0$ and pH should be studied in their positive and negative (+ 1:-1) levels, respectively. In that case, increasing factor A ($[U]_0$) and decreasing C (pH) will lead to higher values of Y_1.

The contour plot for removal percentage of hydroxyapatite considering $[U]_0$ and adsorbent dosage, shown in Fig. 4(b), displays that the level is much higher at the

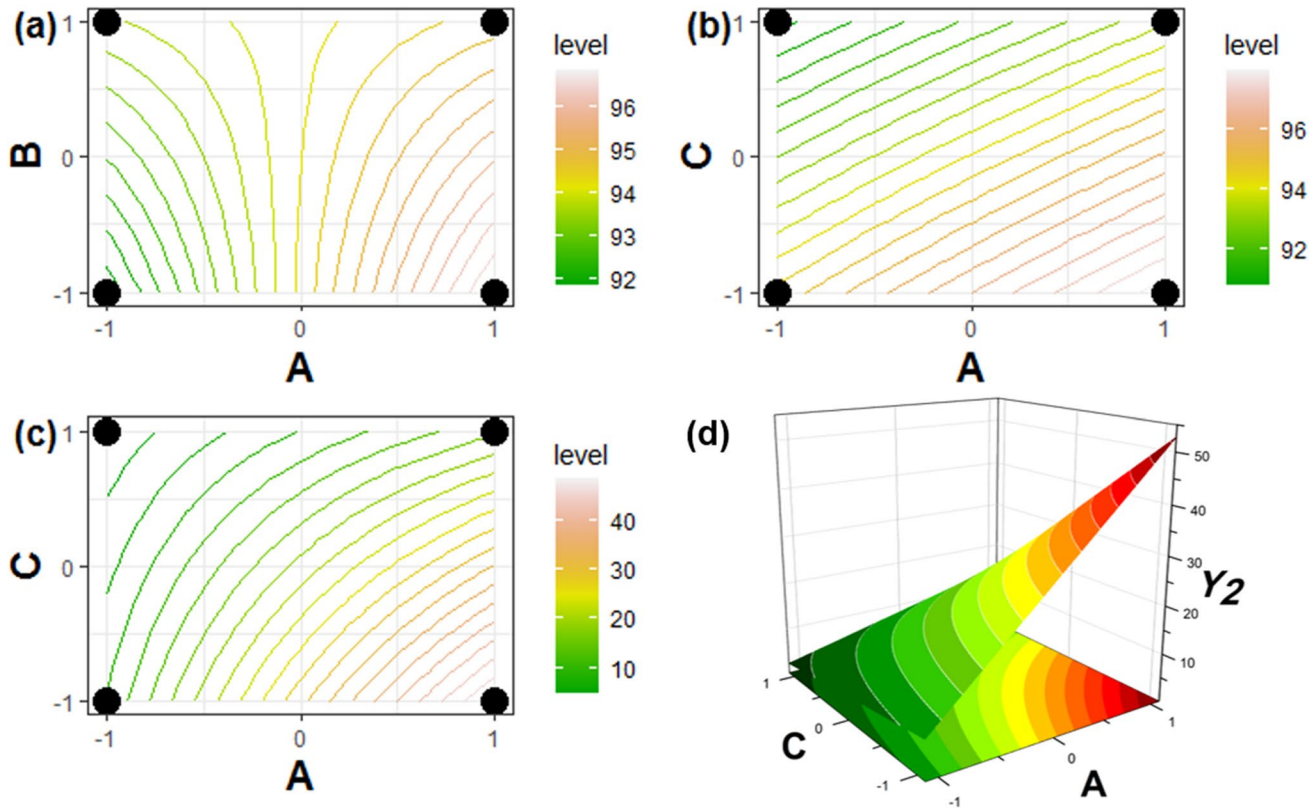


Fig. 4 Contour plot for the experiments with hydroxyapatite. **a** Removal percentage considering variables A:B; **b** removal percentage considering variables A:C; **c** adsorption capacity; **d** response surface graph of A:C: Y_2 (adsorption capacity, mg g^{-1})

right-hand inferior diagonal. In real-world values, $[U]_0$ should be set up at 500 mg L^{-1} and $M = 5$ g L^{-1}.

Figure 4c and 4d shows a fast increase in the hydroxyapatite adsorption capacity (Y_2) with increasing $[U]_0$ (A) and decreasing M (C), meaning that one should increase uranium concentration and diminish adsorbent mass to further explore the experimental domain and search for higher values of Y_2. These results indicate the potential of this material, being necessary fewer dosages than those used (< 5 g L^{-1}) to reach its maximum capacity. Because the interaction between A:C was statistically significant to the response, only the solution's initial concentration (mg L^{-1}) and M (g L^{-1}) were considered in the contour plot (Fig. 4). These plots indicate that the experiments should be taken in $[U]_0 = 500$ mg L^{-1} and $M = 5$ g L^{-1} to obtain the maximum q value. In the case of uranium removal, the most important interaction effect is observed for A:B ($[U]_0$:pH) (Fig. 4a), whereas for the adsorption capacity, A:C ($[U]_0$:adsorbent dosage) was the most important one (Fig. 4c).

The statistical summary (see Supplementary Information, Tables S3 and S4) and the Pareto charts (Fig. 5) show the significant effects on the responses at the 95% confidence level (p values < 0.05) for the experiments with bone meal.

The significant terms regarding uranium removal (%) by bone meal were different than those with hydroxyapatite. The interaction effects were the most important factors in this scenario, indicating the negative effect of the interaction A:B ($[U]_0$:pH) and the positive effect of the three-way interaction A:B:C ($[U]_0$:pH:dosage). Although the statistical data had presented these effects in quantitative terms, care must be taken since the values of uranium removal (R, %) were very close, with all the values being higher than 99%.

As regards the adsorption capacity of uranium by bone meal, the results were similar to those observed for hydroxyapatite, i.e., positive effect of $[U]_0$ and negative effect of adsorbent dosage and their interaction (Table S4). As also seen for hydroxyapatite, this material was able to uptake more uranium with the increase in $[U]_0$.

Figure 6a illustrates the two-dimensional contour plot for the response variable Y_4, while Fig. 6b displays the surface response for bone meal considering the combined effects A:C.

Figure 6a shows similar behavior to that of Fig. 4c, in which bone meal adsorption capacity for uranium (Y_2) is rapidly boosted with increasing $[U]_0$ (A) and decreasing M (C). Greater values of adsorption capacity are expected with increasing element concentrations, especially when removal

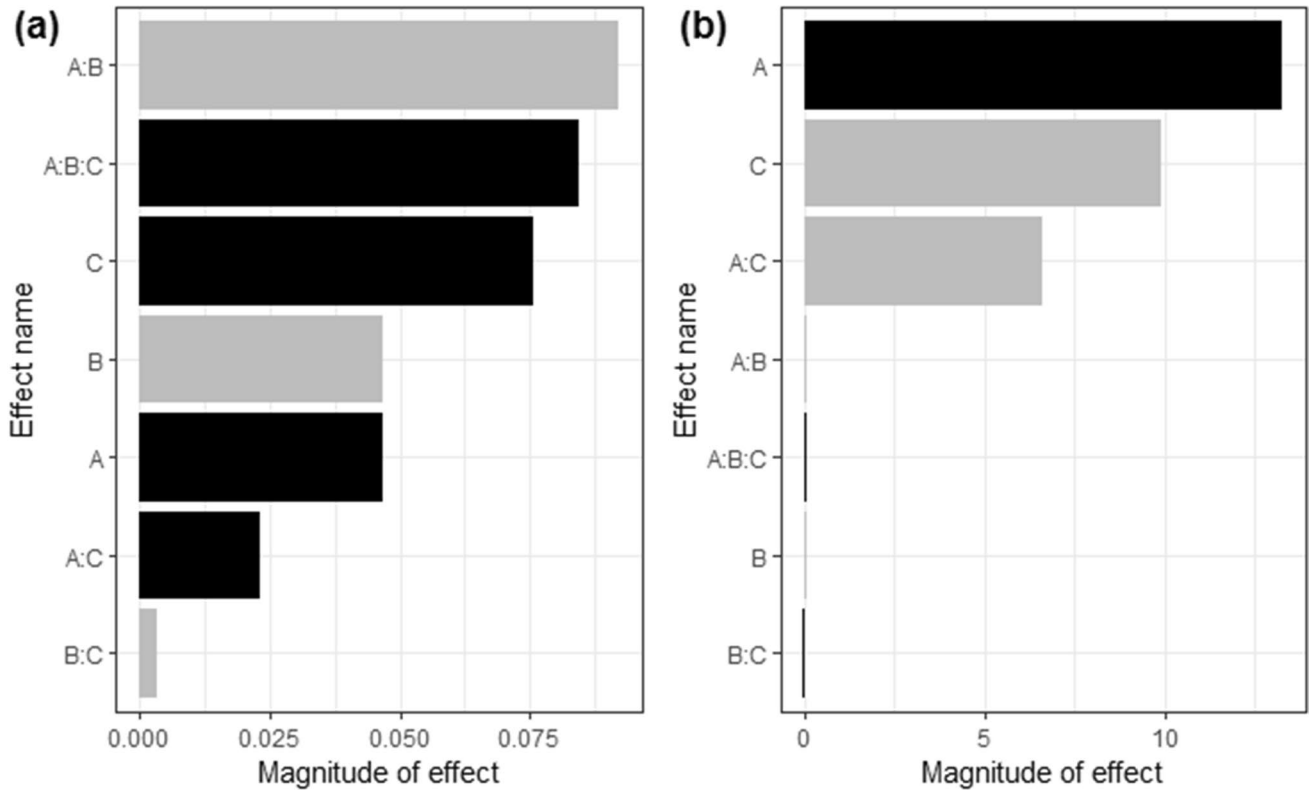


Fig. 5 Pareto plots for the experiments with bone meal: (gray fill) negative effect, (black fill) positive effect. **a** Removal percentage; **b** adsorption capacity. A = $[U]_0$, B = pH, C = M (g L^{-1})

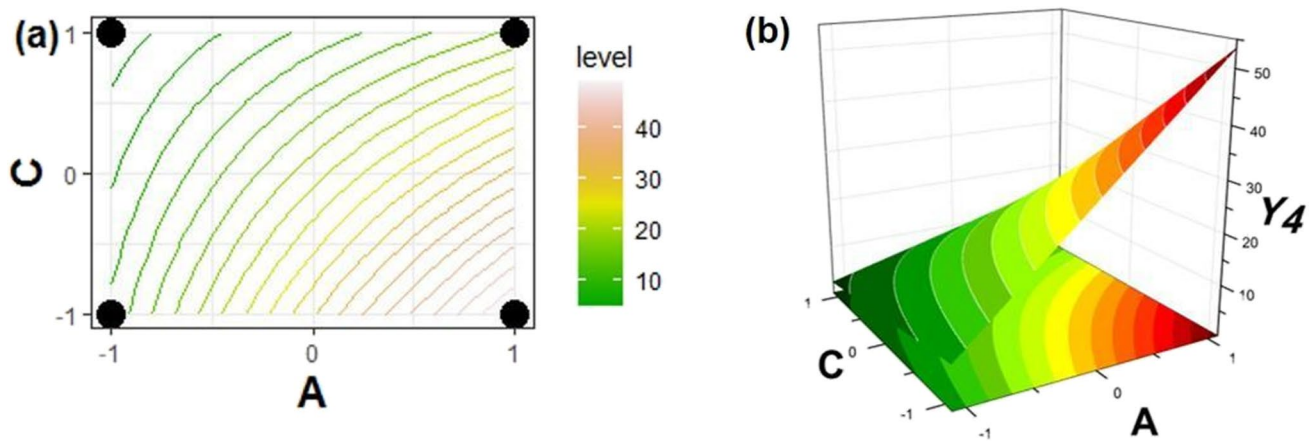


Fig. 6 Contour plot for the experiments with bone meal. **a** Adsorption capacity considering variables A:C. **b** Response surface graph of A:C:Y_4 (adsorption capacity, mg g^{-1})

is high in any studied experimental condition. The rationale is that when the ratio of adsorbent mass and volume of solution is fixed, the q values are very dependent on the relation between initial and final element concentrations. For this reason, when the biosorbent is still able to uptake the target element, q tends to increase. For both materials, for assessing their maximum capacities, one should increase uranium concentration and reduce the amounts of the adsorbents per volume of solution. The contour plot of removal percentage for the experiments with the bone meal was omitted considering that all the performed experiments reveal more than 99.5% of the uranium removal percentage. The comparison between the experimental data and predicted values for adsorption capacity are given in Table S5. The results

demonstrate that the experimental and the predicted data were in good agreement, with an $R^2 = 0.99934$.

Application in a liquid radioactive organic waste

Both hydroxyapatite and bone meal were evaluated as biosorbents of a LORW. The experiments were conducted in the collected LORW, as received (AR). The $[U]_0$ in the LORW-AR is within the range of uranium concentration studied in the experimental design with the synthetic solutions ($[U]_0$ approx. 220 mg L^{-1}). Again, $M = 5$ g L^{-1} and 15 g L^{-1} were evaluated. The results show that these adsorbents performed very similarly (adsorption capacity of approximately 22 mg g^{-1} for both materials) and experiments with less adsorbent dosage provided the best results. Although bone meal achieved a greater U removal percentage with the prepared solutions, hydroxyapatite ($q = 22.11$ mg g^{-1}, removal = 99.34%) presented the best results for LORW in terms of adsorption capacity. The final pH for the materials slightly increased from about 3 to the range of 3.07–3.69.

The equations generated from the full factorial experimental design (Table 4) were applied to predict the removal behavior of U in LORW. The experimental and the predicted data (Table S6) revealed that the estimated values of U removal through these equations provided similar results to those obtained in the experiments, indicating that these equations can satisfactorily predict this system even if applied to a complex radioactive organic waste. This is a clear indication of the adsorption selectivity achieved for these biosorbents in the experimental conditions, given that the presence of other radionuclides and organic compounds did not hamper their performance.

Comparison with the literature

The comparison of the experimental adsorption capacity (q_{exp}, mg g^{-1}) of hydroxyapatite and bone meal with adsorption capacities of several adsorbents for uranium in previous studies are displayed in Table 5 (See also Supplementary Information, Fig. S2).

As shown in Table 5 and Fig. S4a, hydroxyapatite and bone meal presented better results than many materials, such as *Yarrowia lipolytica* marine yeast, *Solanum incanum* leaves, *Pistia stratiotes*, sugar beet pulp, *Citrus lemon* peels, *Chlamydomonas* sp., and live *Pseudomonas* strain, but clearly, there are other biosorbents with higher adsorption capacities for the treatment of synthetic solutions contaminated with uranium, such as pomegranate peel, *Aspergillus nidulans*, *Ankistrodesmus* sp., cyanobacterium *Anabaena flos-aquae*, *Sargassum boveanum*, *Lemna* sp., *Russula sanguinea*, *Cladophora hutchinsiae*, *Vigna radiata*, *Ceratophyllum demersum*, *Cystoseira* sp., and *Eichhornia crassipes*. A cluster of these biosorbents is shown in Fig. S3b and indicates that hydroxyapatite and bone meal are in the same aggregate of the *Solanum incanum* leaves, $H_2O_2/MgCl_2$-treated *Azolla filiculoides*, pomegranate peel, and the brown algae *Laminaria japonica* (if 4 groups are considered for the entire clustering set).

Conversely, when real radioactive waste solutions are considered, the studied materials presented better results than most materials. *Lemna* sp., for instance, presented a q_{exp} of 162 mg g^{-1} when applied to synthetic solutions. This value is much higher than those obtained for the bone meal (49.87 mg g^{-1}) and hydroxyapatite (49.20 mg g^{-1}). On the other hand, when employed in the treatment of LORW, both bone meal and hydroxyapatite presented about 10 times the adsorption capacities of *Lemna* sp. However, when compared to Quercetin-sodium hydroxide modified *Spirulina Platensis*, these values were 3.3 times lower. Given that the materials used in the present work have not yet been modified to increase their potentials, the so-far obtained results are promising.

As mentioned by Satir et al. (2021) and Hariani et al. (2019), bone meal and hydroxyapatite have many benefits. They are natural or synthesized from natural sources, are environmentally sound and inexpensive. Given that these materials were similar in terms of adsorption capacities and uranium removal, bone meal is more cost-attractive since it is easily obtained. Moreover, bone meal does not require to be synthesized, and is more affordable.

Conclusions

The adsorption capacity to remove uranium from aqueous solution by bone meal and hydroxyapatite was evaluated in this work. A two-level full factorial design was used for modeling and optimization of uranium removal conditions. The optimization experiments had to be carried out with a [U] of 500 mg L^{-1} and 0.05 g of the biosorbent, so to obtain the highest adsorption performance towards U present in an aqueous solution. Under these conditions, hydroxyapatite was able to remove 98.5% of U, with a q of 49.2 mg g^{-1}. In the case of bone meal, a removal of 99.9% and a q of 49.9 mg g^{-1} were achieved. The findings indicated that bone meal and hydroxyapatite offer a potentially efficient and cost-effective alternative in the treatment of aqueous solutions containing U, but also demonstrated real application in the treatment of complex solutions such as liquid organic radioactive waste (LORW), having achieved over 99% of U removal. In this scenario, hydroxyapatite achieved the highest uranium uptake (22.11 mg g^{-1}). The obtained results on the removal of U in LORW by these materials revealed that the presence of other radionuclides and organic compounds did not alter their efficiency. Moreover, the empirical model developed in the present work was able

Table 5 Comparison of uranium uptake by several biomasses with those used in the present work

Biomass	Type of solution	q (mg g^{-1})	Reference
Bone meal	Synthetic	49.87	This work
	Radioactive liquid organic waste	22.08	
Hydroxyapatite	Synthetic	49.20	
	Radioactive liquid organic waste	22.11	
H_2O_2/$MgCl_2$-treated *Azolla filiculoides*	Synthetic	42.2	Namdarian et al. (2021)
Ca-pretreated *Cystoseira indica* algae	Synthetic	454.50	Hassan Khani et al. (2006)
Brown algae *Laminaria japonica*	Synthetic	96.4	Lee et al. (2014)
Sargassum biomass	Synthetic	560	Yang and Volesky (1999)
Pomegranate peel	Synthetic	93.4	Nuhanović et al. (2021)
Aspergillus nidulans	Synthetic	263.16	Abozaid et al. (2021)
Ankistrodesmus sp.	Synthetic	601.2	Cheng et al. (2021)
Quercetin-sodium hydroxide modified *Spirulina Platensis*	Real radioactive waste	73	Mohammed (2020)
Cyanobacterium *Anabaena flos-aquae*	Synthetic	196.4	Yuan et al. (2020)
Sargassum boveanum	Synthetic	255	Hashemi et al. (2020)
Yarrowia lipolytica marine yeast	Synthetic	15.11	Kolhe et al. (2020)
Solanum incanum leaves	Synthetic	39.98	Bakather et al. (2020)
Rice and coffee husks	Radioactive liquid organic waste	1.96	Ferreira et al. (2020)
Pistia stratiotes	Synthetic	6.81	Vieira et al. (2019)
Lemna sp.	Synthetic	162.08	
	Radioactive liquid organic waste	2.20	
Sugar beet pulp	Synthetic	20.45	Nuhanović et al. (2019)
Citrus lemon peels	Synthetic	24.39	Šabanović et al. (2019)
Chlamydomonas sp.	Synthetic	6.34	Baselga-Cervera et al. (2018)
Russula sanguinea	Synthetic	174.3	Bağda et al. (2018)
Raw coconut fiber	Real radioactive waste	0.66	Ferreira et al. (2018)
Activated coconut fiber	Real radioactive waste	1.82	Ferreira et al. (2018)
Cladophora hutchinsiae	Synthetic	152	Bağda et al. (2017)
Vigna radiata	Synthetic	230	Naeem et al. (2017)
Ceratophyllum demersum	Synthetic	140.45	Yi et al. (2017)
Cystoseira sp.	Synthetic	468.01	Gök et al. (2017)
Eichhornia crassipes	Synthetic	142.8	Yi et al. (2016)
Potamogeton pectinatus L	Synthetic	1.56	Pratas et al. (2014)
Lyophilized *Pseudomonas* strain	Synthetic	0.54	Sar and D'Souza (2001)
Live *Pseudomonas* strain	Synthetic	0.41	Sar and D'Souza (2001)

to satisfactorily predict the values of q and R, suggesting a high affinity of these materials for uranium. In addition, the adsorption capacity found for these adsorbents was relatively higher in comparison with other reported materials for the removal of U.

Supplementary Information The online version contains supplementary material available at https://doi.org/10.1007/s11356-021-17551-x.

Acknowledgements The authors acknowledge the fellowship awarded by the Brazilian National Council for Scientific and Technological Development to TW. We also thank the support given by the Center for Lasers and Applications' Multiuser Facility at IPEN-CNEN/SP in the SEM/EDS analysis, and Dr. Flavia R.O. Silva and Dr. Rafael V.P. Ferreira for supplying the hydroxyapatite and the bone meal, respectively.

Author contribution TW: data curation, investigation, resources, visualization, writing—original draft. SNG: formal analysis, resources, writing—review and editing. JTM: conceptualization, funding acquisition, supervision, writing—review and editing. RPS: investigation. LGA: conceptualization, formal analysis, methodology, project administration, resources, visualization, writing—review and editing.

All authors read and approved the final manuscript.

Funding This project was supported by the Nuclear and Energy Research Institute, the Brazilian National Council for Scientific and Technological Development, and the Brazilian National Nuclear Energy Commission.

Data Availability All data generated or analyzed during this study are included in this published article and its supplementary information.

Declarations

Ethics approval and consent to participate Not applicable.

Consent for publication Not applicable.

Competing interests The authors declare no competing interests.

References

Abbas SH, Ismail IM, Moustafa TM et al (2014) Biosorption of heavy metals: a review. J Chem Sci Technol 3:74–102

Abozaid SM, Shetaia YM, Rabie KA, et al (2021) Recovery of uranium from solutions using *Aspergillus nidulans* isolated from monazite mineral Int J Environ Anal Chem 1–31https://doi.org/10.1080/03067319.2021.1939022

Ahmed W, Núñez-Delgado A, Mehmood S, et al (2021) Highly efficient uranium (VI) capture from aqueous solution by means of a hydroxyapatite-biochar nanocomposite: adsorption behavior and mechanism Environ Res 201https://doi.org/10.1016/j.envres.2021.111518

Akkaya R (2012) Thermodynamic parameters of TI^{+}, Ra^{2+}, Bi^{3+} and Ac^{3+} adsorption onto polyhydroxyethylmethacrylate-hydroxyapatite composite. J Radioanal Nucl Chem 292:771–775. https://doi.org/10.1007/s10967-011-1513-0

Ashry A, Bailey EH, Chenery SRN et al (2016) Kinetic study of time-dependent fixation of U^{VI} on biochar. J Hazard Mater 320:55–66. https://doi.org/10.1016/j.jhazmat.2016.08.002

Bağda E, Sarı A, Tuzen M (2018) Effective uranium biosorption by macrofungus (*Russula sanguinea*) from aqueous solution: equilibrium, thermodynamic and kinetic studies. J Radioanal Nucl Chem 317:1387–1397. https://doi.org/10.1007/s10967-018-6039-2

Bağda E, Tuzen M, Sarı A (2017) Equilibrium, thermodynamic and kinetic investigations for biosorption of uranium with green algae (*Cladophora hutchinsiae*). J Environ Radioact 175–176:7–14. https://doi.org/10.1016/j.jenvrad.2017.04.004

Bakather OY, Zouli N, Abutaleb A et al (2020) Uranium (VI) ions uptake from liquid wastes by *Solanum incanum* leaves: Biosorption, desorption and recovery. Alexandria Eng J. https://doi.org/10.1016/j.aej.2020.03.013

Baselga-Cervera B, Romero-López J, García-Balboa C et al (2018) Improvement of the uranium sequestration ability of a Chlamydomonas sp. (ChlSP strain) isolated from extreme uranium mine tailings through selection for potential bioremediation application. Front Microbiol 9:523. https://doi.org/10.3389/fmicb.2018.00523

Bayoumi TA, Saleh HM (2018) Characterization of biological waste stabilized by cement during immersion in aqueous media to develop disposal strategies for phytomediated radioactive waste. Prog Nucl Energy 107:83–89. https://doi.org/10.1016/j.pnucene.2018.04.021

Bayoumi TA, Saleh HM, Eskander SB (2013) Solidification of hot real radioactive liquid scintillator waste using cement-clay composite. Monatshefte Fur Chemie 144:1751–1758. https://doi.org/10.1007/s00706-013-1065-9

Chen C, Hu J, Wang J (2020) Biosorption of uranium by immobilized *Saccharomyces cerevisiae*. J Environ Radioact 213:106158. https://doi.org/10.1016/j.jenvrad.2020.106158

Chen S, Hong J, Yang H et al (2013) Adsorption of uranium (VI) from aqueous solution using a novel graphene oxide-activated carbon felt composite. J Environ Radioact 126:253–258. https://doi.org/10.1016/j.jenvrad.2013.09.002

Cheng Y, Li F, Liu N et al (2021) A novel freeze-dried natural microalga powder for highly efficient removal of uranium from wastewater. Chemosphere 282:131084. https://doi.org/10.1016/j.chemosphere.2021.131084

Coelho E, Reis TA, Cotrim M et al (2020) Bioremediation of water contaminated with uranium using *Penicillium piscarium*. Biotechnol Prog. https://doi.org/10.1002/btpr.3032

Coutelot FM, Seaman JC, Baker M (2018) Uranium (VI) adsorption and surface complexation modeling onto vadose sediments from the Savannah River Site. Environ Earth Sci 77:148. https://doi.org/10.1007/s12665-018-7316-7

Curtis GP, Fox P, Kohler M et al (2004) Comparison of in situ uranium K_D values with a laboratory determined surface complexation model. Appl Geochemistry 19:1643–1653. https://doi.org/10.1016/j.apgeochem.2004.03.004

Das N (2010) Recovery of precious metals through biosorption - a review. Hydrometallurgy 103:180–189. https://doi.org/10.1016/j.hydromet.2010.03.016

Das N (2012) Remediation of radionuclide pollutants through biosorption - an overview. Clean - Soil, Air, Water 40:16–23. https://doi.org/10.1002/clen.201000522

Davis JA, Meece DE, Kohler M et al (2004) Approaches to surface complexation modeling of Uranium (VI) adsorption on aquifer sediments. Geochim Cosmochim Acta 68:3621–3641. https://doi.org/10.1016/j.gca.2004.03.003

Dong L, Yang J, Mou Y et al (2017) Effect of various environmental factors on the adsorption of U (VI) onto biochar derived from rice straw. J Radioanal Nucl Chem 314:377–386. https://doi.org/10.1007/s10967-017-5414-8

Dunn K (2021) pid: Process Improvement using Data. R package version 0.50. https://CRAN.R-project.org/package=pid. Accessed 08 October 2021

Ferreira EGA, Alves E, Ferreira RVP et al (2015) Biosorption of thorium by bone meal. WM Symposia, Phoenix, USA

Ferreira EGA, Ferreira RVP, Araujo LG, et al (2013) Chemical analysis of radioactive mixed liquid wastes by chemical analysis of radioactive mixed liquid wastes by alpha/gamma spectrometry, ICP-OES and Arsenazo III.

Ferreira RVP, Araujo LG, Canevesi RLS et al (2020) The use of rice and coffee husks for biosorption of U (total), ^{241}Am, and ^{137}Cs in radioactive liquid organic waste. Environ Sci Pollut Res Int. https://doi.org/10.1007/s11356-020-09727-8

Ferreira RVP, Silva EA, Canevesi RLS et al (2018) Application of the coconut fiber in radioactive liquid waste treatment. Int J Environ Sci Technol 15:1629–1640. https://doi.org/10.1007/s13762-017-1541-6

Foster RI, Amphlett JTM, Kim KW et al (2020) SOHIO process legacy waste treatment: Uranium recovery using ion exchange. J Ind Eng Chem 81:144–152. https://doi.org/10.1016/j.jiec.2019.09.001

Gök C, Aytas S, Sezer H (2017) Modeling uranium biosorption by *Cystoseira sp*. and application studies. Sep Sci Technol 52:792–803. https://doi.org/10.1080/01496395.2016.1267212

Guilhen SN, Coleti J, Tenório JAS et al (2019) Influence of adsorption parameters on uranium adsorption capability by biochar derived from macauba coconut residue. Braz J Radiat Sci 07(2A):01–14. https://doi.org/10.15392/bjrs.v7i2A.590

Guilhen SN, Rovani S, Araujo LG et al (2021) Uranium removal from aqueous solution using macauba endocarp-derived biochar: Effect of physical activation. Environ Pollut 272:116022. https://doi.org/10.1016/j.envpol.2020.116022

Hadjittofi L, Pashalidis I (2014) Uranium sorption from aqueous solutions by activated biochar fibres investigated by FTIR

spectroscopy and batch experiments. J Radioanal Nucl Chem 304:897–904. https://doi.org/10.1007/s10967-014-3868-5
Hariani PL, Muryati M, Said MS (2019) Kinetic and thermodynamic adsorption of nickel (II) onto hydroxyapatite prepared from Snakehead (*Channastriata*) fish bone. Mediterr J Chem 9:85–94. https://doi.org/10.13171/mjc92190906825plh
Hashemi N, Dabbagh R, Noroozi M, Baradaran S (2020) Optimization of uranium biosorption in solutions by *Sargassum boveanum* using RSM method. 9:65–84. https://doi.org/10.12989/aer.2020.9.1.065
Hassan Khani M, Reza Keshtkar A, Meysami B, FirouzZarea M, Jalali R (2006) Biosorption of uranium from aqueous solutions by nonliving biomass of marine algae *Cystoseira indica* Electron J Biotechnol 9. https://doi.org/10.2225/vol9-issue2-fulltext-8
I. Puigdomenech, HYDRA (hydrochemical Equilibrium Constant Database) and MEDUSA (make Equilibrium Diagrams Using Sophisticated Algorithms) Programs, Royal Institute of Technology, Sweden. (2006). http://www.kemi.kth.se/medusa/. Accessed 06 October 2021
Kahouli S (2011) Re-examining uranium supply and demand: new insights. Energy Policy 39:358–376. https://doi.org/10.1016/j.enpol.2010.10.007
Kim H, Um W, Kim WS et al (2017) Synthesis of tributyl phosphate-coated hydroxyapatite for selective uranium removal. Ind Eng Chem Res 56:3399–3406. https://doi.org/10.1021/acs.iecr.6b04491
Kim J, Sambudi NS, Cho K (2019) Removal of Sr^{2+} using high-surface-area hydroxyapatite synthesized by non-additive in-situ precipitation. J Environ Manage 231:788–794. https://doi.org/10.1016/j.jenvman.2018.10.100
Kolhe N, Zinjarde S, Acharya C (2020) Removal of uranium by immobilized biomass of a tropical marine yeast *Yarrowia lipolytica*. J Environ Radioact 223–224:106419. https://doi.org/10.1016/j.jenvrad.2020.106419
Kong L, Ruan Y, Zheng Q et al (2020) Uranium extraction using hydroxyapatite recovered from phosphorus containing wastewater. J Hazard Mater 382:120784. https://doi.org/10.1016/j.jhazmat.2019.120784
Lee KY, Kim KW, Baek YJ, Chung DY, Lee EH, Lee SY, Moon JK (2014) Biosorption of uranium (VI) from aqueous solution by biomass of brown algae *Laminaria japonica*. Water Sci Technol 70:136–143. https://doi.org/10.2166/wst.2014.205
Liu J, Zhao C, Zhang Z et al (2016) Fluorine effects on U(VI) sorption by hydroxyapatite. Chem Eng J 288:505–515. https://doi.org/10.1016/j.cej.2015.12.045
Mishra V, Sureshkumar MK, Gupta N et al (2017) Study on sorption characteristics of uranium onto biochar derived from eucalyptus wood. Water Air Soil Pollut 228:309. https://doi.org/10.1007/s11270-017-3480-8
Mohammed AAER (2020) Potentiality of quercetin-sodium hydroxide modified *Spirulina Platensis* in uranium biosorption from waste effluent. Int J Environ Stud 77:48–60. https://doi.org/10.1080/00207233.2019.1688988
Naeem H, Bhatti HN, Sadaf S et al (2017) Uranium remediation using modified *Vigna radiata* waste biomass. Appl Radiat Isot 123:94–101. https://doi.org/10.1016/j.apradiso.2017.02.027
Namdarian N, Tajer Mohammad Ghazvini P, TabatabaeeBafroee AS (2021) Bio-removal of uranium by the treated biosorbent from aqueous solutions as an efficient strategy in uranium bioremediation. Appl Biol 34:163–177. https://doi.org/10.22051/JAB.2020.33051.1378
Nuhanović M, Grebo M, Draganović S et al (2019) Uranium(VI) biosorption by sugar beet pulp: equilibrium, kinetic and thermodynamic studies. J Radioanal Nucl Chem 322:2065–2078. https://doi.org/10.1007/s10967-019-06877-z
Nuhanović M, Smječanin N, Mulahusić N et al (2021) Pomegranate peel waste biomass modified with H_3PO_4 as a promising sorbent for uranium(VI) removal. J Radioanal Nucl Chem 328:617–626. https://doi.org/10.1007/s10967-021-07664-5
Ouassel S, Chegrouche S, Nibou D et al (2021) Application of response surface methodology for uranium (VI) adsorption using hydroxyapatite prepared from eggshells waste material: Study of influencing factors and mechanism. Water Sci Technol 83:1198–1216. https://doi.org/10.2166/wst.2021.022
Pang C, Liu YH, Cao XH et al (2011) Biosorption of uranium (VI) from aqueous solution by dead fungal biomass of *Penicillium citrinum*. Chem Eng J 170:1–6. https://doi.org/10.1016/j.cej.2010.10.068
Paterlini V, Bettinelli M, Rizzi R et al (2020) Characterization and luminescence of Eu^{3+} - and Gd^{3+} - Doped hydroxyapatite $Ca_{10}(PO_4)_6(OH)_2$. Curr Comput-Aided Drug Des 10:806. https://doi.org/10.3390/cryst10090806
Pratas J, Paulo C, Favas PJC et al (2014) Potential of aquatic plants for phytofiltration of uranium-contaminated waters in laboratory conditions. Ecol Eng 69:170–176. https://doi.org/10.1016/j.ecoleng.2014.03.046
R Core Team (2021). R: A language and environment for statistical computing. R Foundation for Statistical Computing, Vienna, Austria. URL https://www.R-project.org/. Accessed 23 July 2021
Rosenberg E, Pinson G, Tsosie R et al (2016) Uranium remediation by ion exchange and sorption methods: a critical review. Johnson Matthey Technol Rev 60:59–77. https://doi.org/10.1595/205651316X690178
Šabanović E, Muhić-Šarac T, Nuhanović M et al (2019) Biosorption of uranium (VI) from aqueous solution by *Citrus limon* peels: kinetics, equlibrium and batch studies. J Radioanal Nucl Chem 319:425–435. https://doi.org/10.1007/s10967-018-6358-3
Saleh HM, Moussa HR, El-Saied FA et al (2020) Mechanical and physicochemical evaluation of solidified dried submerged plants subjected to extreme climatic conditions to achieve an optimum waste containment. Prog Nucl Energy 122:103285. https://doi.org/10.1016/j.pnucene.2020.103285
Sar P, D'Souza SF (2001) Biosorptive uranium uptake by a *Pseudomonas strain*: characterization and equilibrium studies. J Chem Technol Biotechnol 76:1286–1294. https://doi.org/10.1002/jctb.517
Satir IT, Ozdemir N, Donmez Gungunes CD (2021) Bone meal and chitosan biocomposite: a new biosorbent for the removal of Victoria Blue R from wastewater Chem Eng Commun 1–15https://doi.org/10.1080/00986445.2021.1957850
Sprynskyy M, Kowalkowski T, Tutu H et al (2011) Adsorption performance of talc for uranium removal from aqueous solution. Chem Eng J 171:1185–1193. https://doi.org/10.1016/j.cej.2011.05.022
Vieira LC, Araujo LG, Ferreira RVP et al (2019) Uranium biosorption by *Lemna* sp. and *Pistia stratiotes*. J Environ Radioact 203:179–186. https://doi.org/10.1016/j.jenvrad.2019.03.019
Wang J, Chen C (2006) Biosorption of heavy metals by *Saccharomyces cerevisiae*: A review. Biotechnol Adv 24:427–451. https://doi.org/10.1016/j.biotechadv.2006.03.001
Wang J, Chen C (2009) Biosorbents for heavy metals removal and their future. Biotechnol Adv 27:195–226. https://doi.org/10.1016/j.biotechadv.2008.11.002
Wang JS, Hu XJ, Liu YG et al (2010) Biosorption of uranium (VI) by immobilized *Aspergillus fumigatus* beads. J Environ Radioact 101:504–508. https://doi.org/10.1016/j.jenvrad.2010.03.002
Wang J, Zhuang S (2019) Extraction and adsorption of U (VI) from aqueous solution using affinity ligand-based technologies: an overview. Rev Environ Sci Biotechnol 18:437–452. https://doi.org/10.1007/s11157-019-09507-y
Wang S, Guo W, Gao F et al (2018) Lead and uranium sorptive removal from aqueous solution using magnetic and nonmagnetic fast pyrolysis rice husk biochars. RSC Adv 8:13205–13217. https://doi.org/10.1039/c7ra13540h

Xiong T, Li Q, Liao J, Zhang Y, Zhu W (2021) Highly enhanced adsorption performance to uranium (VI) by facile synthesized hydroxyapatite aerogel. J Hazard Mater 423B:127184. https://doi.org/10.1016/j.jhazmat.2021.127184

Yakout SME, Abdeltawab AA, Elhindi K et al (2018) Uranium dynamic adsorption breakthrough curve onto rice straw based activated carbon using bed depth service time model. BioResources 13:9143–9157. https://doi.org/10.15376/biores.13.4.9143-9157

Yang J, Volesky B (1999) Biosorption of uranium on *Sargassum* biomass. Water Res 33:3357–3363. https://doi.org/10.1016/S0043-1354(99)00043-3

Yi ZJ, Yao J, Chen HL et al (2016) Uranium biosorption from aqueous solution onto *Eichhornia crassipes*. J Environ Radioact 154:43–51. https://doi.org/10.1016/j.jenvrad.2016.01.012

Yi ZJ, Yao J, Zhu MJ et al (2017) Biosorption characteristics of *Ceratophyllum demersum* biomass for removal of uranium (VI) from an aqueous solution. J Radioanal Nucl Chem 313:19–27. https://doi.org/10.1007/s10967-017-5269-z

Younes AA, Masoud AM, Taha MH (2018) Uranium sorption from aqueous solutions using polyacrylamide-based chelating sorbents. Sep Sci Technol 53:2573–2586. https://doi.org/10.1080/01496395.2018.1467450

Yuan Y, Liu N, Dai Y et al (2020) Effective biosorption of uranium from aqueous solution by cyanobacterium *Anabaena flos-aquae*. Environ Sci Pollut Res 27:44306–44313. https://doi.org/10.1007/s11356-020-10364-4

Zhang J, Chen X, Zhou J et al (2020) Uranium biosorption mechanism model of protonated *Saccharomyces cerevisiae*. J Hazard Mater 385:121588. https://doi.org/10.1016/j.jhazmat.2019.121588

Zhang XT, Jiang DM, Xiao YQ, Chen JC, Xia LS (2019) Adsorption of uranium (VI) from aqueous solution by modified rice stem. J Chem. https://doi.org/10.1155/2019/6409504

Zhao C, Liu J, Yuan G et al (2018) A novel activated sludge-graphene oxide composites for the removal of uranium (VI) from aqueous solutions. J Mol Liq 271:786–794. https://doi.org/10.1016/j.molliq.2018.09.069

Publisher's Note Springer Nature remains neutral with regard to jurisdictional claims in published maps and institutional affiliations.